

RESEARCH

Open Access



# Fractality of The Geysers

A. Sakhaee-Pour\*

\*Correspondence:  
sakhaee@ou.edu  
Petroleum and Geological  
Engineering, The University  
of Oklahoma, Norman, OK,  
USA

## Abstract

Heat convection at pore-scale, which is strongly dependent on the topology of pore space, remains poorly understood for geothermal reservoirs. This is despite fundamental advances made in modeling heat transfer in nano- and micro-scale conduits. With this in mind, we analyze the fractality of the pore space of The Geysers to fully characterize its topology. We consider circular and slit-like throat geometries to represent aspect ratios close to unity and infinity, respectively. Our study shows that the effective length of pore space follows the general fractal rule. This study can have major implications for understanding heat convection at pore-scale by presenting a representative fractal model for The Geysers.

**Keywords:** The Geysers, Fractal dimension, Acyclic pore model

## Background

Geothermal resources are a part of the U.S. energy portfolio for moving toward a cleaner energy system, according to the Department of Energy Strategic Plan for 2014–2018. The largest operating geothermal reservoir is The Geysers located in the US. Other countries in Europe (Arola et al. 2014; Schintgen 2015; Rolker et al. 2015) and Asia (Kong et al. 2014; Singh et al. 2014) also explored the possibility of using geothermal reservoirs at large scale. Improving energy recovery from geothermal reservoirs (Jain et al. 2015) is possible by gaining a better understanding of the energy transfer through these environmentally friendly resources.

Heat transfer through convection to the flowing fluid is dependent on geometrical features, such as wetting surface and residing time (Bird et al. 2007). There have been major advances in understanding physics of the heat transfer for a single conduit at small scale (Guo and Zhao 2005; Pinson et al. 2007; Laguerre et al. 2008) but applications of such understanding remained limited to synthetic pore space where the topology of the pores is well described (Magnico 2009), or simplified (Willingham et al. 2008). One of the main reasons for the lack of knowledge in the area of heat transfer at pore-scale, unlike fluid flow which is fairly developed, is the absence of a realistic pore model that can be easily incorporated with our basic knowledge in heat transfer.

Void space and solid grains (non-void regions) constitute the porous medium. We suppose that the void space is not a continuum medium distributed over the entire rock in the pore-scale modeling approach. The pore-scale models classify the void space into pores, or pore bodies, and pore throats, and then investigate the interactions between

the pores. The interactions between the pores occur through the pore throats, which are often considered the narrowest region of the void space between two neighboring pores. The spatial distribution of the throats and their characteristic size control the transport properties.

There are few theoretical pore models that account for the effective connectivity of the pore space at core scale. The characteristic size of the pore is usually on the order of microns or smaller, while the size of the core is close to few centimeters. The difference between the two sizes underscores the importance of upscaling from the small scale to the large scale. The upscaling phenomenon is a well-known problem in transport phenomena with few analytical models for the effective connectivity of the pore space. The scarcity of theoretical models implies the difficulty of finding realistic theoretical models. Pore models that are solely based on high-resolution images are limited to a small region of the porous medium, much smaller than the size of a core, and they are not necessarily relevant to the effective connectivity at the core scale.

The first theoretical pore model was invented nearly a century ago when bundle of tubes were used to represent the void space inside a porous medium (Washburn 1921). The bundle-of-tubes model was crucial for the development of the field of pore-scale modeling because its simplicity was appealing (Purcell 1949). Researchers have revised the bundle-of-tubes model to account for the fractal features of pore space (Cai et al. 2010; Cai and Yu 2011), which allow them to capture imbibition more accurately. The next theoretical pore model appeared three decades later when the interconnectivity of pores was included by using a regular lattice model (Fatt 1956). Sphere-packing, or pack of beads, also accounted for the interconnectivity of pores based on the hypothesis that the random distribution of the spheres is representative of grains or sedimentary rocks (Finney 1968).

The notion of interconnectivity with random distribution of the spheres was crucial for explaining different transport properties of porous media, such as two-phase permeability (Bryant and Blunt 1992), three-phase permeability (Blunt 2001), drainage (Mason and Mellor 1995; Prodanovic and Bryant 2006), gelation in porous media (Thompson and Fogler 1997, 1998), and the flow of non-Newtonian fluids (Balhoff and Thompson 2004, 2006), especially for unconsolidated sands (Harris and Morrow 1964). This notion which led to the random distribution of the pore size on the network is not necessarily realistic for tight formations (Mousavi and Bryant 2012). The spatially random distribution of pore size leads to a plateau-like trend of capillary pressure with wetting phase saturation which was used for explaining percolation in porous media (Sahimi 1994). The plateau-like trend is usually absent in tight gas sandstones (Prodanovic et al. 2013; Mehmani and Prodanovic 2014).

The present author, with his colleague, developed two theoretical pore models for the effective connectivity of the pore space in tight formations (Sakhaee-Pour and Bryant 2014). The effective connectivity of pore space in tight gas sandstones can be modeled using a multi-type model which embraces regular lattice and tree-like configurations. For shales (Sakhaee-Pour and Bryant 2012; Kethireddy et al. 2014; Eshkalak et al. 2014; Saneifar et al. 2015; Yu and Sepehrnoori 2014; Qajar et al. 2015), we can use the acyclic pore model (Sakhaee-Pour and Bryant 2015) in which there is a single path between any two points in the pore space. The acyclic pore model can be characterized by using

fractal rules which can provide a convenient basis for understanding transport phenomena at pore-scale.

Fractals, which are self-similar patterns, provide convenient mathematical bases for describing complex features; this is one of the reasons that they find different applications. Examples of such applications are diverse, ranging from globalization (Karpiarz et al. 2014), to ultra-stiff materials (Oftadeh et al. 2014), to superfluid turbulence (Kivontides et al. 2001), and to earthquakes (Sahimi et al. 1992). They have also been used for analyzing transport in porous media (Mandelbrot 1983; Katz and Thompson 1985; Radlinski et al. 1999; Coleman and Vassilicos 2008). The general rule of fractals is that the total volume and the length are related to the characteristic size as follows:

$$L(\delta) \propto \delta^{1-D_l} \quad (1a)$$

$$V(\delta) \propto \delta^{3-D'_l}, \quad (1b)$$

where  $L$  is the fractal length,  $\delta$  is the characteristic size,  $D_l$  is the fractal dimension that controls the length,  $V$  is the volume, and  $D'_l$  is the fractal dimension that controls the volume. These equations are often referred to as the general scaling rules of the fractals.

Researchers have also used the general fractal rule to describe tortuous porous media. For this reason, they accounted for tortuosity as follows (Cai et al. 2010; Cai and Yu 2011):

$$L_f(\delta) = L_s^{D_T} \delta^{1-D_T}, \quad (2)$$

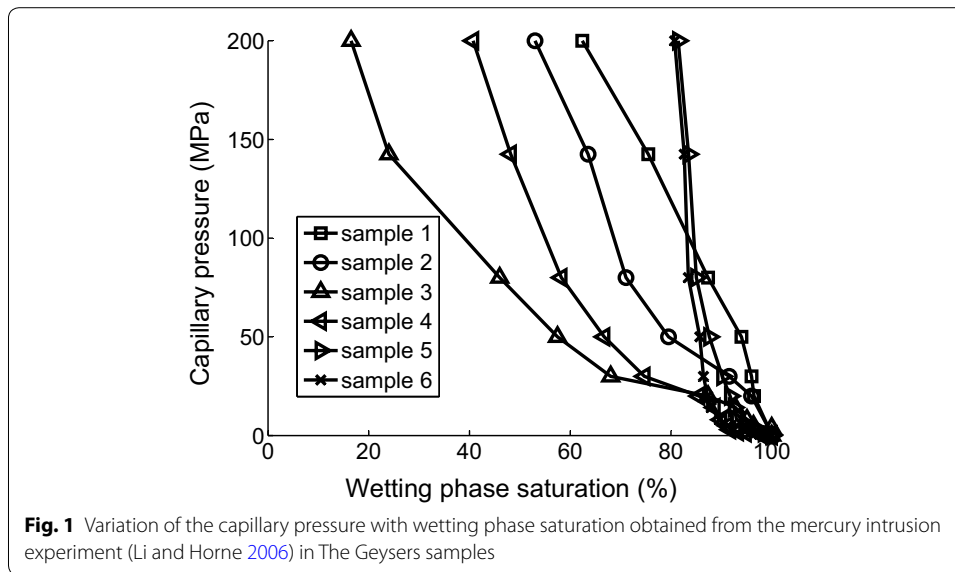
where  $L_f$  is the actual length of the pore space in which flow travels,  $L_s$  is the straight-line distance between the traveled points, and  $D_T$  is the tortuosity fractal dimension. The ratio of the two lengths defines tortuosity ( $= [L_f/L_s]^2$ ). The tortuous fractal model simplifies to the bundle-of-tubes model when the tortuosity fractal dimension is equal to unity. The tortuous model for the pore length ( $L_p$ ) becomes identical to the general fractal model for length ( $L$ ) if  $L_s^{D_T}$  is a constant coefficient, and tortuosity fractal dimension ( $D_T$ ) is set equal to the fractal dimension that controls the length ( $D_l$ ).

This paper analyzes fractal properties of The Geysers using the general fractal rules (Eqs. 1a, 1b) to characterize its pore space. The drainage data available in the literature will be used for this reason. Our main objective is to determine the fractal dimension of the pore length to build a representative fractal model. We will also compare the fractal dimensions relevant to the pore length ( $D_l$ ) and pore volume ( $D'_l$ ).

## Methods

### Capillary pressure measurements of The Geysers

We turn to analyzing the drainage data of The Geysers samples. Drainage takes place when the non-wetting phase displaces the wetting phase, which is obtained by injecting mercury into the samples (Fig. 1). Mercury is the non-wetting phase to the pore space and air, or mercury vapor, is the wetting phase. The samples were recovered from different wells (Li and Horne 2006) of The Geysers geothermal field, which is the largest geothermal field of the world. The Geysers field is located in Mayacamas Mountains, 72 miles north of San Francisco, California.



The capillary pressure, by definition, is equal to the difference between the pressures of the non-wetting and wetting phases:  $P_c = P_{nw} - P_w$ , where  $P_c$  is the capillary pressure. The subscripts nw and w denote non-wetting and wetting phases, respectively. This definition lets us relate the capillary pressure to the mercury pressure by assuming negligible wetting phase pressure. The wetting phase saturation is also determined from mercury volume injected into the sample at each capillary pressure as follows:

$$S_w = 1 - S_{nw} = 1 - \frac{V_{Hg}}{V_p}, \quad (3)$$

where  $S_w$  is the wetting phase saturation,  $S_{nw}$  is the non-wetting phase saturation,  $V_{Hg}$  is the volume of mercury injected into the sample, and  $V_p$  is the pore volume.

## Results and discussion

### Fractality of The Geysers

We investigate fractality of the pore volumes of The Geysers samples whose drainage data are shown in Fig. 1. For this purpose, we analyze the variation of the total pore volume invaded at each capillary pressure, with the characteristic size of the pore space. The pore volume invaded at each capillary pressure is equal to the mercury volume injected into the sample and its pore size is determined using the Young–Laplace relation as follows:

$$P_c = P_{nw} - P_w = \sigma C \cos(\theta), \quad (4)$$

where  $C$  is the curvature,  $\sigma$  is the interfacial tension between the phases, and  $\theta$  is the contact angle between the two phases. The curvature is a geometrical parameter:  $C = 2/r$  for circular, and  $1/h$  for slit-like conduits in which  $r$  is the radius of the throat and  $h$  is the height of the slit.

Figure 2 shows variation of pore volume with throat radius. We list the corresponding fractal dimensions of the samples, which agree with the data in the literature, in Table 1.

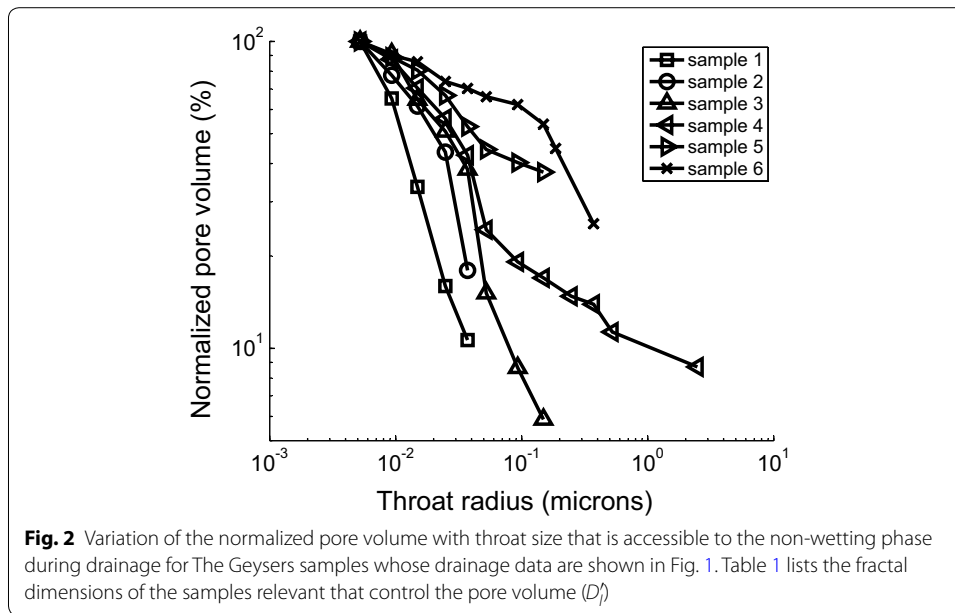


**Table 1** Fractal dimensions of The Geysers samples whose capillary pressure measurements are shown in Fig. 1. The range of the length scale used for fractal characterization is also listed

Sample#	1	2	3	4	5	6
Name (Li and Horne 2006)	SB15D_1	MLM_3	Pc_92	SB15D_2	PRATI_5	CA1862_4
$D_f'$ (Li and Horne 2006)	4.12	4.069	3.957	3.483	3.224	3.188
$D_f'$	4.196	3.802	3.917	3.451	3.326	3.268
$D_{f-circular}$	3.891	3.176	3.529	3.364	2.905	2.764
$D_{f-slit}$	2.895	2.386	2.657	2.388	1.985	1.862
Range of length scale ( $\mu\text{m}$ )	(0.010, 0.074)	(0.010, 0.074)	(0.010, 0.297)	(0.010, 4.954)	(0.010, 0.297)	(0.010, 0.746)

The results are normalized versus total pore volume. The calculations are based on the premise that the accessibility of the pore volume is controlled by capillarity. No assumption is invoked for the effective connectivity of the pore space; thus, the results are relevant to the pore volume and the transport properties relevant to the flow.

In the present study, we determine the fractal dimension relevant to the pore volume using a single fitting parameter (Eq. 1b) by accounting for the volume of non-wetting phase injected. However, the values reported in the literature (Li and Horne 2006) are based on capturing capillary pressure measurements using three fitting parameters in a model that is identical to the Brooks–Corey model (1964) when the fractal dimension is smaller than three. The difference between the numbers of parameters can lead to the difference observed between the fractal dimensions ( $D_f$ ) listed in Table 1 for each sample.

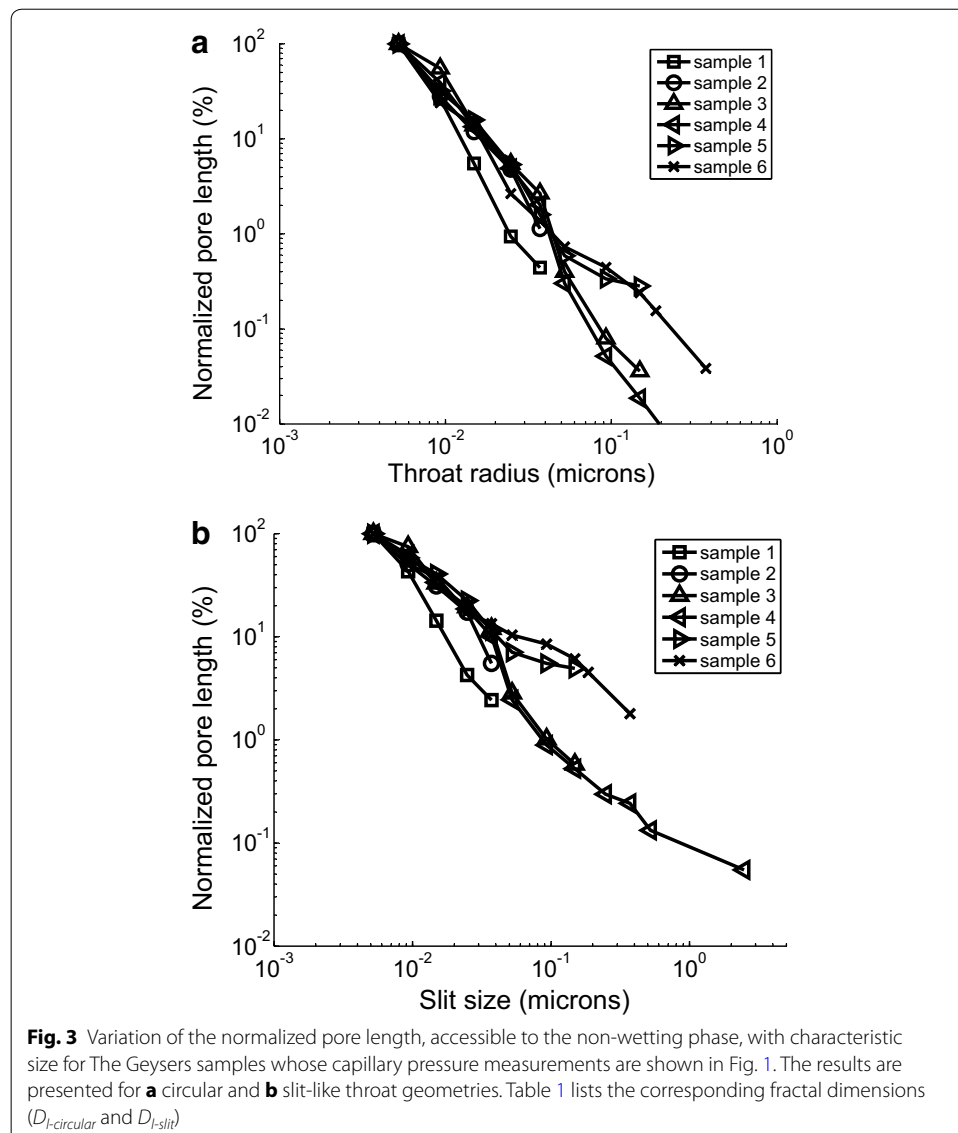
Next, we suppose that the pore space of The Geysers can be captured using a connected network of circular or slit-like conduits. We denote the characteristic sizes of circular and slit-like conduits by  $r$  and  $h$ , respectively. Hence, we model the total pore volume invaded during the drainage as follows:

$$V_{\text{Hg}} = \sum_i \Delta V_{\text{nw}} \propto \sum_i r_i^2 l_i \quad \text{circular} \tag{5a}$$

$$V_{\text{Hg}} = \sum_i \Delta V_{\text{nw}} \propto \sum_i h_i l_i \quad \text{slit-like} \tag{5b}$$

where  $V_{\text{Hg}}$  is the mercury volume injected into the sample, the subscript  $i$  denotes the capillary pressure increment,  $r_i$  is the radius of the circular conduit,  $h_i$  is the height of the slit, and  $l_i$  is the corresponding length of the conduit. The characteristic size of the conduit ( $r_i$  or  $h_i$ ) is dependent on the capillary pressure based on the Young–Laplace equation (Eq. 4).

Now, we investigate fractality of the pore length of The Geysers. For this purpose, we first determine the total pore length obtained from Eq. 5a and normalize the results for the sake of comparison. Figure 3 shows that the total pore length follows the general



scaling rule of the fractals whose fractal dimensions are listed in Table 1. The results are more compatible with the general scaling rule compared to the pore volume presented in Fig. 2.

The fractal dimensions in this study are determined using a statistical multiple non-linear regression model (Mendenhall et al. 1989). The accuracy of this model is measured based on the multiple coefficient of determination,  $R^2$ , where  $0 \leq R^2 \leq 1$ . Table 2 lists this coefficient for the fractal dimensions relevant to the pore volume and pore length. This coefficient is larger than or equal to 0.96 for the pore length, indicating the compatibility of the model with the fractal general rule. This number decreases when evaluated for the pore volume, which indicates its deviation from the fractal general rule.

Our analysis indicates that the fractal dimension of the network of slit-like conduits is smaller than that of the circular conduits for each sample. Compare  $D_{l-circular}$  with  $D_{l-slit}$  in Table 1. The difference between the fractal dimensions suggests that the pore length of the slit-like pores is smaller than that of the pores whose aspect ratios are close to unity for a given characteristic size. This can have major implications for predicting heat transfer through heat convection at pore-scale in The Geysers. The heat convection is dependent on the wetting surface and residing time. The wetting surface is dependent on the pore length, while the residing time is dependent on the characteristic size of the conduit controlling the flow conductance.

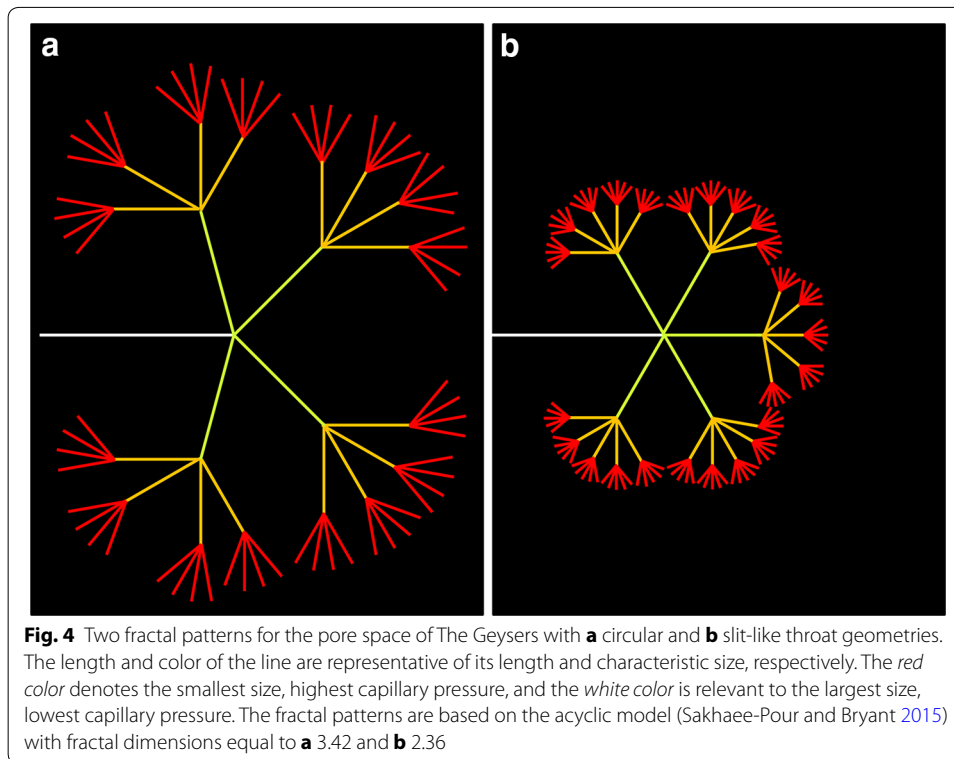
Table 1 reveals that the fractal dimension is dependent on whether we use pore volume or pore length for our analysis even in a single pore model.  $D'_p$ , which is based on the analysis of the pore volume, is different from the fractal dimensions obtained from the pore length ( $D_{l-circular}$  and  $D_{l-slit}$ ). Thus, using a single fractal dimension for describing different aspects of the pore space of the geothermal resource is not accurate.

The fractal dimension is an indicator of the complexity of a topology. The greater complexity corresponds to the greater heterogeneity of pore space. The fractal dimension that controls the pore volume ( $D'_p$ ) is always larger than that of the pore length ( $D_{l-circular}$  and  $D_{l-slit}$ ) for the samples analyzed. This tells us that the heterogeneity of the pore volume is greater than that of the pore length. Thus, transport properties that are more dependent on the pore volume, instead of pore length, are envisaged to be more dependent on the spatial location in The Geysers.

We present two fractal patterns for the pore space of The Geysers. We take the fractal dimensions to be equal to 3.42 and 2.32 for the circular and slit-like conduits, respectively. These numbers are close to the average of the fractal dimensions listed. It is also easy to construct acyclic models (Bethe 1935; Sakhaee-Pour and Bryant 2015) for them. We start with a line of unit length (white line in Fig. 4), which is often referred to as the initiator (Feder 2013). We then generate four branches (green lines) whose lengths

**Table 2** Coefficients of non-linear regressions for the pore volume and pore length of each sample

Sample	1	2	3	4	5	6
$R^2(D'_p)$	0.98	0.87	0.93	0.94	0.97	0.86
$R^2(D_{l-circular})$	0.99	0.99	0.98	0.98	0.97	0.98
$R^2(D_{l-slit})$	0.99	0.96	0.96	0.96	0.97	0.98



are two-third of the initiator for the circular conduits, and repeat this process two more times. The fractal dimension of the generated topology, as shown in Fig. 4a, is equal to  $3.42 (= \log [4] / \log [1.5])$ .

We also generate a fractal pattern for the slit-like geometry. We begin with a line of unit length similar to the circular throat geometry (white line in Fig. 4b). We then generate 5 branches whose lengths are half of the initiator, and repeat this process for two more times. This creates a fractal pattern whose dimension is equal to  $2.32 (= \log[5] / \log[2])$ .

The characteristic size of the pores is on the order of few nanometers to micrometers in The Geysers samples (Fig. 2). High-resolution images are required to capture the void space of these samples, and such images are usually limited to an extremely small volume of the rock. The fractal patterns presented here, on the other hand, are based on the drainage experiments conducted on core plugs whose sizes are usually on the order of few centimeters. It is not yet possible to build a pore model based on the high-resolution images to capture the effective connectivity of the pore space at the large scale ( $\sim 1$  cm). Thus, it is not yet possible to test the developed model using high-resolution images.

Figure 4 shows the fractal patterns of the pore space of The Geysers. The presented patterns shed light on the pore length and the characteristic size of the representative pore models. The length of the line represents the pore length and its color denotes the characteristic size. The red color shows the smallest size, highest capillary pressure; the white color shows the largest size, lowest capillary pressure, which are included in the illustrations. The difference between the presented topologies indicates the difference between the total lengths of the pore models. We should emphasize that the pore models



are not unique simply because fractals do not possess a unique representation for a given fractal dimension. The presented patterns aim to clarify the importance of considering different geometries for the cross-sectional area of the pore space.

## Conclusions

Our main objective in this study was to analyze the fractality of pore space of The Geysers. For this purpose, we considered circular and slit-like conduits to mimic aspect ratios close to unity and infinity, respectively. We realized that the fractal dimension of the pore space that controls the pore length is close to 3.4 if we use circular conduits to capture the void space. If we use slit-like conduits instead, the fractal dimension reduces to 2.3. Our analysis also shows that the fractal dimension of the geothermal reservoir depends on whether we analyze the pore volume or the pore length. We presented fractal patterns for the pore length of The Geysers using the acyclic pore model. The presented models for the pore length can have major implications for understanding heat convection at pore-scale.

## Competing interests

The author declares that he has no competing interests.

Received: 12 September 2015 Accepted: 4 January 2016

Published online: 16 January 2016

## References

- Arola T, Eskola L, Hellen J, Korhonen-Niemi K. Mapping the low enthalpy geothermal potential of shallow Quaternary aquifers in Finland. *Geotherm Energy*. 2014;2(1):1–20.
- Balhoff MT, Thompson KE. Modeling the steady flow of yield-stress fluids in packed beds. *AIChE J*. 2004;50(12):3034–48.
- Balhoff MT, Thompson KE. A macroscopic model for shear-thinning flow in packed beds based on network modeling. *Chem Eng Sci*. 2006;61(2):698–719.
- Bethe HA. Statistical theory of superlattices. *Proc. Roy. Soc. Lond*. 1935;150(871):552–75.
- Bird RB, Stewart WE, Lightfoot EN. *Transport phenomena*. New York: John Wiley; 2007.
- Blunt MJ. Flow in porous media—pore-network models and multiphase flow. *Curr Opin Coll Interface Sci*. 2001;6(3):197–207.
- Brooks RH, Corey AT. Properties of porous media affecting fluid flow. *J Irrigat Drain Div*. 1966;92(2):61–90.
- Bryant S, Blunt M. Prediction of relative permeability in simple porous media. *Phys Rev*. 1992;46(4):2004–5.
- Cai J, Yu B, Zou M, Luo L. Fractal characterization of spontaneous co-current imbibition in porous media. *Energy Fuels*. 2010;24(3):1860–7.
- Cai J, Yu B. A discussion of the effect of tortuosity on the capillary imbibition in porous media. *Transp Porous Media*. 2011;89(2):251–63.
- Coleman SW, Vassilicos JC. Tortuosity of unsaturated porous fractal materials. *Phys Rev*. 2008;E78(1):016308.
- Eshkalak MO, Al-Shalabi EW, Sanaei A, Aybar U, Sepehrnoori K. Simulation study on the CO<sub>2</sub>-driven enhanced gas recovery with sequestration versus the re-fracturing treatment of horizontal wells in the US unconventional shale reservoirs. *J Nat Gas Sci Eng*. 2014;21:1015–24.
- Fatt I. The network model of porous media I. Capillary pressure characteristics. *AIME Pet Trans*. 1956;207:144–59.
- Feder J. *Fractals*. Berlin: Springer; 2013.
- Finney J. Random packing and the structure of the liquid state. Dissertation, University of London. 1998.
- Guo Z, Zhao TS. A lattice Boltzmann model for convection heat transfer in porous media. *Numer Heat Transf*. 2005;47(2):157–77.
- Harris CC, Morrow NR. Pendular moisture in packings of equal spheres. *Nature*. 1964;203:706–8.
- Jain C, Vogt C, Clauser C. Maximum potential for geothermal power in Germany based on engineered geothermal systems. *Geotherm Energy*. 2015;3(1):1–20.
- Karpiarz M, Fronczak P, Fronczak A. International trade network: fractal properties and globalization puzzle. *Phys Rev Lett*. 2014;113(24):248701.
- Katz A, Thompson AH. Fractal sandstone pores: implications for conductivity and pore formation. *Phys Rev Lett*. 1985;54(12):1325.
- Kethireddy N, Chen H, Heidari Z. Quantifying the effect of kerogen on electrical resistivity measurement in organic-rich source rocks. *Petrophysics*. 2014;55(3):136–46.
- Kivotides D, Vassilicos JC, Barenghi CF, Khan MAI, Samuels DC. Quantum signature of superfluid turbulence. *Phys Rev Lett*. 2001;87(27):275302.

- Kong Y, Pang Z, Shao H, Hu S, Kolditz O. Recent studies on hydrothermal systems in China: a review. *Geotherm Energy*. 2014;2(1):1–12.
- Laguerre O, Ben Amara S, Alvarez G, Flick D. Transient heat transfer by free convection in a packed bed of spheres: comparison between two modelling approaches and experimental results. *Appl Therm Eng*. 2008;28(1):14–24.
- Li K, Horne RN. Fractal modeling of capillary pressure curves for The Geysers rocks. *Geothermics*. 2006;35(2):198–207.
- Magnico P. Pore-scale simulations of unsteady flow and heat transfer in tubular fixed beds. *AIChE J*. 2009;55(4):849–67.
- Mandelbrot BB. *The Fractal Geometry of Nature*. London: Macmillan; 1983.
- Mason G, Mellor DW. Simulation of drainage and imbibition in a random packing of equal spheres. *J Coll Interface Sci*. 1995;176(1):214–25.
- Mehmani A, Prodanovic M. The effect of microporosity on transport properties in porous media. *Adv Water Resour*. 2014;63:104–19.
- Mendenhall W, Reinmuth JE, Beaver R. *Statistics for Management and Economics*. Boston: PWS-Kent Publishing Company; 1989.
- Mousavi MA, Bryant SL. Connectivity of pore space as a control on two-phase flow properties of tight-gas sandstones. *Transp Porous Media*. 2012;94(2):537–54.
- Oftadeh R, Haghpanah B, Vella D, Boudaoud A, Vaziri A. Optimal fractal-like hierarchical honeycombs. *Phys Rev Lett*. 2014;113(10):104301.
- Pinson F, Gregoire O, Quintard M, Prat M, Simonin O. Modeling of turbulent heat transfer and thermal dispersion for flows in flat plate heat exchangers. *Int J Heat Mass Transf*. 2007;50(7):1500–15.
- Prodanovic M, Bryant SL. A level set method for determining critical curvatures for drainage and imbibition. *J Coll Interface Sci*. 2006;304(2):4422–58.
- Prodanovic M, Bryant SL, Davis JS. Numerical simulation of diagenetic alteration and its effect on residual gas in tight gas sandstones. *Transp Porous Media*. 2013;96(1):39–62.
- Purcell WR. Capillary pressures—their measurement using mercury and the calculation of permeability therefrom. *J Pet Technol*. 1949;1(02):39–48.
- Qajar A, Daigle H, Prodanovic M. Methane dual-site adsorption in organic-rich shale-gas and coalbed systems. *Int J Coal Geol*. 2015;149:1–8.
- Radlinski AP, Radlinska EZ, Agamalian M, Wignall GD, Lindner P, Randl OG. Fractal geometry of rocks. *Phys Rev Lett*. 1999;82(15):3078.
- Rolker J, Schill E, Stober I, Schneider J, Neumann T, Kohl T. Hydrochemical characterization of a major central European heat flux anomaly: the Bürcchau geothermal spring system, Southern Black Forest Germany. *Geotherm Energy*. 2015;3(1):1–18.
- Sahimi M, Robertson MC, Sammis CG. Relation between the earthquake statistics and fault patterns, and fractals and percolation. *Phys A: Stat Mech Appl*. 1992;191(1):57–68.
- Sahimi M. *Applications of percolation theory*. Bristol, PA : Taylor & Francis; 1994.
- Sakhaee-Pour A, Bryant SL. Gas permeability of shale. *SPE Reserv Eval Eng*. 2012;15(4):401–9.
- Sakhaee-Pour A, Bryant SL. Effect of pore structure on the producibility of tight-gas sandstones. *AAPG Bull*. 2014;98(4):663–94.
- Sakhaee-Pour A, Bryant SL. Pore structure of shale. *Fuel*. 2015;143:467–75.
- Saneifar M, Aranibar A, Heidari Z. Rock classification in the Haynesville shale based on petrophysical and elastic properties estimated from well logs. *SEG Interpret*. 2015;3(1):SA65–75.
- Schintgen T. Exploration for deep geothermal reservoirs in Luxembourg and the surroundings—perspectives of geothermal energy use. *Geotherm Energy*. 2015;3(1):1–30.
- Singh HK, Kumar Y, Chandrasekharam D, Gurav T, Singh B. High-heat-producing granites of East Dharwar Craton around Gugi, Karnataka, and their possible influence on the evolution of Rajapur thermal springs, Deccan Volcanic Province India. *Geotherm Energy*. 2014;2(1):1–12.
- Thompson KE, Fogler HS. Pore-level mechanisms for altering multiphase permeability with gels. *SPE J*. 1997;2(03):350–62.
- Thompson KE, Fogler HS. Pore-scale model for fluid injection and in situ gelation in porous media. *Phys Rev*. 1998;E57(5):5825–32.
- Washburn EW. The dynamics of capillary flow. *Phys Rev*. 1921;17(3):273.
- Willingham TW, Werth CJ, Valocchi AJ. Evaluation of the effects of porous media structure on mixing-controlled reactions using pore-scale modeling and micromodel experiments. *Environ Sci Technol*. 2008;42(9):3185–93.
- Yu W, Sepehrnoori K. Simulation of gas desorption and geomechanics effects for unconventional gas reservoirs. *Fuel*. 2014;116:455–64.